Journal of Applied Polymer Science

Shaping PEDOT nanoparticles for use in 3D tissue phantoms

Elizabeth M. Wailes,[1,2*] Christopher M. MacNeill,[1*] Eleanor McCabe,[1] Nicole H. Levi-Polyachenko[1,2]

[1]Department of Plastic and Reconstructive Surgery, Wake Forest University School of Medicine, Medical Center Blvd, Winston Salem North Carolina 27157

[2]Virginia Tech-Wake Forest School of Biomedical Engineering and Sciences, Wake Forest University, 575 N. Patterson Avenue, Winston Salem North Carolina 27101

Elizabeth M. Wailes and Christopher M. MacNeill contributed equally to this work.

Correspondence to: N.H. Levi-Polyachenko (E-mail: nlevi@wakehealth.edu)

ABSTRACT: Controlling the relative concentrations of surfactant, oxidant iron (III) chloride, 3,4-ethylenedioxythiophene (EDOT) monomer in water, and mechanical influences such as sonication and stirring, resulted in the synthesis of PEDOT nanoparticles with various dimensions and aspect ratios. Having a ratio of two or more of surfactant compared to the oxidant led to a greater yield of thinner nanofibers, as did utilizing a more dilute concentration of the reactants. These nanoparticles were shown to be cytocompatible in 3D culture for both human and mouse cells. The key feature is that PEDOT nanoparticles with a variety of morphologies can be obtained using water only without the need for hexanes in the procedures. The synthesized PEDOT nanoparticles absorb light across the infrared spectrum and in turn are capable of generating heat for biologically relevant studies of hyperthermia in three dimensional tissue phantoms. © 2016 Wiley Periodicals, Inc. J. Appl. Polym. Sci. **2016**, *133*, 43378.

KEYWORDS: bioengineering; conducting polymers; nanoparticles; nanowires and nanocrystals; self-assembly

Received 24 August 2015; accepted 22 December 2015

DOI: 10.1002/app.43378

INTRODUCTION

Initially used exclusively as films, PEDOT is often blended with polystyrene sulfonate (PSS) for enhanced solubility. Recently, PEDOT has been synthesized into water-soluble dispersions of nanoparticles.[1–6] PEDOT nanofibers can be custom made using a hard template method to control nucleation and growth, but this method can require large investments in technology.[7] It would be advantageous to be able to make a variety of sizes and shapes in a simple manner because both overall size and relative dimensions (aspect ratio) govern particle properties, including optical and electrical effects for displays, and with biological applications such as synthetic cell interfaces, administration of heat, and pharmaceutical therapy.[7–12]

Soft template methods take advantage of the thermodynamic equilibrium of catonic, anionic, or non-ionic solute concentrations.[3] Surfactants, such as sodium dodecylsulfate (SDS) or sodium bis (2-ethylhexyl) sulfosuccinate (AOT), can be used to generate a micellar template, and the shape of the micelles is dependent upon the hydrophobic nature of the material, solvents, and concentrations used.[13] AOT has been shown by *Z*hang *et al.*, to be useful in the synthesis of PEDOT nanotubes.[5] Following similar procedures, we proposed that SDS, which is a larger and longer-chained surfactant, with a higher aspect ratio (relative to AOT) might promote high aspect ratio particle formation, as shown in Schematic 1. The synthesis procedures described below utilize chemical oxidation polymerization using iron chloride as the oxidizing agent and SDS as the micelle template. Previously, it has been shown that the shape of PEDOT nanoparticles was dependent upon the amount of aqueous iron chloride to hexane, with higher ratios yielding nanotubes.[8] Yoon *et al.*, explored the ratios of aqueous iron chloride to EDOT to hexane, with the highest percentage of nanotubes achieved with higher amounts of water and iron chloride used.[8] Paradee and Sirivat synthesized multiple distinct shapes of PEDOT nanoparticles using an aqueous soft template with peroxydisulfate (APS) as the oxidant, including raspberries, coralliform, orange peel, plum and globular shapes.[14] Following similar protocols, we wished to make nanotubes and NF from PEDOT by adapting aqueous based protocols instead of hexane in order to avoid one source of potential cytotoxicity.

Hyperthermic temperatures above 45 °C lead to irreversible denaturation of proteins. Consequently hyperthermia is often explored in medicine to treat diseases, including the eradication of cancer.[15–19] Alternatively, mild hyperthermia (38–44 °C) has been used to augment drug delivery and wound healing.[20–27] Previous work done by our group has shown that PEDOT nanoparticles can be incorporated into tissue phantoms for

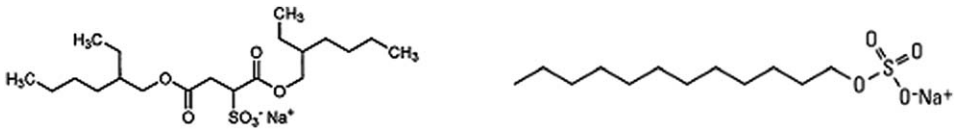

Schematic 1. Chemical structure of sodium bis (2-ethylhexyl) sulfosuccinate (AOT) and sodium dodecylsulfate (SDS).

evaluation of photothermal ablation of cancer cells by capitalizing on the infrared absorption properties inherent in PEDOT.[11] In the previous work, commercially purchased PEDOT ellipsoids were used. The limitations of commercially produced PEDOT nanoparticles include the lack of control over the shape and corresponding optical properties. The most desirable PEDOT nanoparticles for photothermal therapies are those with strong absorption in the near infrared window between 700 and 900 nm, which is an absorption minima for water and hemoglobin.[28] The goal for the current work was to synthesize PEDOT nanofibers (NF) and nanospheres (NS) with strong infrared absorption and the potential for heat generation.

Three- dimensional phantoms provide a means to mimic how cells function and respond to hyperthermia. In addition, there are numerous literature sources documenting that cells cultured in two dimensional conductive substrates have enhanced proliferation and upregulation in the production of cellular communication molecules.[29–34] Cell culture in three dimensions has been shown to be equally or even more sensitive to effects of stimuli than standard two dimension culture.[35–38] Collagen gels are useful as a cost-effective three-dimensional structure in which to evaluate cell manipulation and growth. Like polymer chains, collagen molecules self-assemble to organize and align into nanofibrils. Although other authors have previously demonstrated that PEDOT fibers can be grown directly into soft gels using electrochemical deposition, an alternative means is to dope the gels with nanoparticles formed extrinsically.[39] High aspect ratio nanoparticles composed of conducting materials like PEDOT represent an ideal addition for enhancing low conductivity materials by creating a series of conductive pathways that can overcome percolation thresholds often observed when spherical nanoparticles are utilized. High aspect ratio nanoparticles also interface with collagen fibers and may orient the fibers, which may aid in directing cell growth.

EXPERIMENTAL

Materials

SDS, $FeCl_3$, NaOH, PBS, EDOT, collagenase, PEDOT nanotubes and Pluronic F127 were purchased from Sigma-Aldrich. Collagen I from rat tail was purchased from Corning. Mouse fibroblast (Balb/c CL.7) and human palatal mesenchymal (HEPM) cell lines were purchased from American Type Culture Collection (ATCC) and cultured in Dulbecco's Modified Eagle medium, supplemented with 1% L-glutamine, 1% penicillin/streptomycin and 10% fetal bovine serum. All cells were incubated in a humidified atmosphere of 5% CO_2 at 37 °C in an incubator.

Synthesis of PEDOT Nanoparticles

DI water (10 mL) was added to a 20 mL scintillation vial. SDS was added followed by anhydrous iron (III) chloride in the amounts shown in Table I. The solution was stirred, and in some cases, sonicated using a water bath sonicator. EDOT was then added dropwise and the solution stirred at discrete time/temperature variables as shown in Table I. The solution was centrifuged and re-suspended alternately in water or ethanol for a total of 10 washes to remove residual surfactant and catalyst. The product was vacuum filtered and dried to give the final product. Other parameters were changed for several reactions: syntheses 1–3 were bath sonicated for 30 s immediately before their 30-min spin, and synthesis 7 took place in 15 mL of water instead of the usual 10 mL.

Characterization

The full absorbance spectrum was measured using a Beckman Coulter DU730 Life Science UV/Vis Spectrophotometer and the concentration determined using a standardized concentration curve at 800 nm. Raman spectra were recorded on a DeltaNu Advantage 532 Raman spectrometer at 532 nm. Transmission electron microscopy images were recorded on an FEI Technai

Table I. Experimental Variables Evaluated for Production of PEDOT Nanoparticles Yielding Spheres, Fibers, or Mesh

#	SDS (mg)	$FeCl_3$ (mg)	EDOT (μL)	Spin speed	Sonication	Temp (°C)/Time (h)	Outcome
1	89 [7.4]	24 [2.0]	12 [1]	3	Bath, 30 s	80/3 followed by 20/18	Short fibers
2	90 [3.8]	53 [2.2]	24 [1]	3	Bath, 30 s	80/3 followed by 20/18	Sphere aggregates and some fibers
3	139 [5.8]	50 [2.1]	24 [1]	3	Bath, 30 s	80/3 followed by 20/18	Thin fibers
4	92 [4.6]	43 [2.2]	20 [1]	3	None	80/3 followed by 20/18	Sheets made of large fibers
5	165 [3.3]	82 [1.6]	50 [1]	3	None	80/3 followed by 20/18	Entangled fibers
6	165 [6.6]	50 [2.0]	25 [1]	2.5	None	80/3 followed by 20/18	Long, thin fibers
7	165 [3.3]	84 [1.7]	50 [1]	3	None	80/3 followed by 20/18	Mesh-like fibers
8	325 [6.5]	84 [1.7]	50 [1]	3	None	80/3 followed by 20/18	Spheres

The values in brackets indicate the ratio of SDS or $FeCl_3$ to EDOT.

BioTwin 120 keV TEM with digital imaging. Three hundred μL volumes of aqueous solutions containing PEDOT NF (synthesis 6) or NS (synthesis 8) at concentrations of 0, 1, 10, 100, and 1000 μg/ml were placed into wells of a 48-well plate and the starting temperature measured just prior to application of infrared light. Then, each well was exposed to 3 W of 800 nm light for 60 s, using a continuous wave K-Cube diode laser from K-Laser, USA.

Preparation of Tissue Phantoms

After PEDOT NP syntheses were complete, samples from procedures 6 and 8 (NF and NS) were tested *in vitro* to investigate the cytotoxicity of these particles as a function of aspect ratio and concentration in Balb/c CL.7 and HEPM cells. PEDOT particles and cells were encapsulated in collagen gels by mixing 100 μL 10X PBS, 20 μL 1*M* NaOH, 130 μL of nanoparticle solution in 1X PBS and 1 mg/mL Pluronic® F-127 (a cytocompatible surfactant to aid in distribution of the nanoparticles within the gels), 800 μL of collagen, and 250 μL of cell solution containing 10^6 cells in their appropriate cell culture media. This formulation was added to three wells of a 12-well plate to generate triplicate samples for each variable. The nanoparticle solution had 10 μg/mL, 100 μg/mL, or 1000 μg/mL of the PEDOT particles, or no particles for the control gels. To minimize nanoparticle aggregation, gels were set by first incubating at room temperature for 30 minutes followed by an additional 30 minutes at 37 °C. After the gels were set, fresh media was added and replaced every other day for one week. At the end of the week, the gels were degraded with 2 mg/mL collagenase and the cells were counted using using Trypan blue and a hemocytometer.

Photothermal Ablation of PEDOT Nanoparticles in 3D Gels

PEDOT NF (synthesis 6) or NS (synthesis 8) were tested *in vitro* to assess thermal ablation capacity using similar three-dimensional collagen gels in a 96-well plate with the HEPM cells. PEDOT NP were distributed in collagen gels by mixing 12.5 μL 10×PBS, 2.5 μL 1*M* NaOH, 16.25 μL of nanoparticles in 1 mg/mL Pluronic® F-127 and 1×PBS, 100 μL of 5 mg/mL collagen, and 31.25 μL of 125,000 cells in culture media in each well. The final concentrations of nanoparticles in the gels were 0, 1, 10, or 100 μg/mL. The gels were kept at room temperature for 30 min and then 30 min at 37 °C to allow for the gels to setup then 175 μL of media was added to the gels. The gels were stored in the 37 °C incubator overnight and then laser treated the next day. The laser parameters were 800 nm light, continuous wave, 3 W for 60 s. Gels were laser treated on hot water (42 °C) bottles to maintain the 37 °C temperature outside of the incubator. After laser treatment, gels were incubated for 2 h at 37 °C to allow for cytoplasm fragmentation of the treated cells to completely progress. After 2 h, the gels were degraded with 2 mg/mL collagenase and the cells were counted using Trypan blue and a hemocytometer.

RESULTS AND DISCUSSION

Formation of PEDOT Nanoparticle Shapes

PEDOT molecules can self-organize into a semi-crystalline phase of planar oriented polymer chains.[40,41] In an effort to enhance interfacial surface area, a cylindrical micelle is likely to form to exclude the maximum amount of water, leading to more stable micelles.[8] Under these assumptions, in a completely aqueous system there should be ideal concentrations for forming cylindrical surfactant micelles useful for templating PEDOT nanoparticles. Although soft templating techniques are limited by not being able to have control over the precise morphology of the nanoparticles, the current work eliminates hexane and uses water for both the dissolution of the surfactant and of the oxidant, $FeCl_3$. We hypothesize that it is not water content attributing to the shape variations of the PEDOT NP, as others have suggested when using both water and hexane, but specifically the ratios between the surfactant and $FeCl_3$ as well as overall concentration of the surfactant in water. Whereas other authors using aqueous soft templating have made PEDOT nanoparticles, our synthesis produced the desired NF dependent upon the ratios of the reactants, and processing parameters.[14,41] SDS has an anionic headgroup which ionically binds water, and the hydrophobic tails of SDS orient to form a reverse micelle. The presence of anionic surfactants can improve the conductivity by serving as a counter ion in the PEDOT chains.[13,42] The second variable in controlling aqueously derived PEDOT NP is the ratio of surfactant to iron chloride as the iron cations are thought to alter the molecular packing of the surfactant by increasing the effective area of the headgroup. Our synthesis procedures produced NF and NS only, no nanotubes, because of the use of water only whereas in procedure used to form PEDOT nanotubes, the water displaced the hexane. In all syntheses, the nanoparticles described were gently stirred in an effort to retain the cylindrical micelle template structure, leading to the formation of NF in lieu of spheres. Major differences in nanoparticle morphologies appear to be attributed to the ratios of SDS and $FeCl_3$ and also between SDS and water.

The results from these syntheses are controlled not only by the relative ratios of the constituent chemicals but also by mechanical disruption of the solution. The effects of these processes are shown in Figure 1. Syntheses 1–3 are nearly identical with the exception of their SDS concentrations. However, their products are quite different: the lowest ratio of SDS to EDOT is 3.8 (synthesis 2) and yields spherical aggregates and some fibers, while increasing this ratio to 5.8 (synthesis 3) produces short, thin fibers. Further increasing the ratio to 7.4 (synthesis 1) produces long, thin fibers. When bath sonication is no longer applied, these trends still hold but the ratios between SDS and EDOT do not need to be so high before fibers can be generated. Given the ratios enumerated before, one would expect synthesis 4 to have a few wispy fibers and perhaps some still associating with spherical aggregates. Even though the chemical ratios for synthesis 4 are intermediate between syntheses 2 and 3, its product is much farther along the growth pathway as it yields large sheets made from fibers. This outcome is sensible given that bath sonication during the initial 30 s of template formation in synthesis 1-3 would disrupt the formation of longer templates. As a consequence, it requires a higher concentration of the template molecules before this disruption can be overcome, as demonstrated in synthesis 5. Oftentimes objects larger than 100 nm are excluded from being coined as nanoparticles; however, the diameters of most of the synthesized fibers and spheres are much less than a micron (30–500 nm) and in accordance with

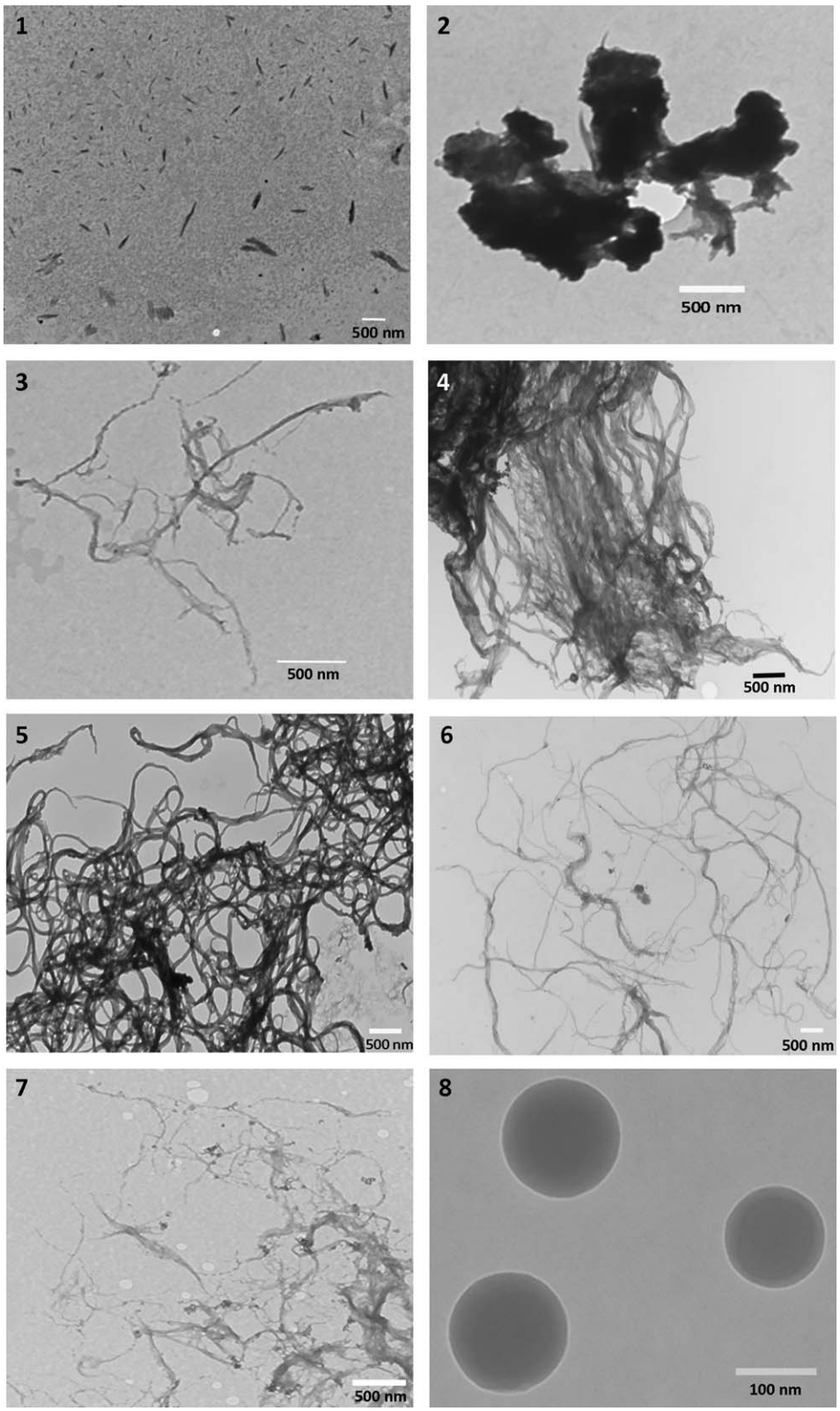

Figure 1. Transmission electron microscopy images of PEDOT nanoparticles synthesized according to the experimental parameters described in Table I. Picture numbers correlate with the synthesis number.

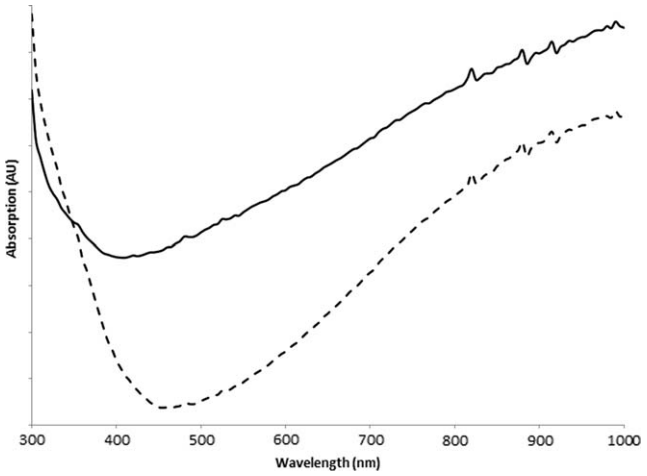

Figure 2. UV-vis absorption spectrum of the synthesized PEDOT NF (solid line) and NS (dashed line) in water.

previous literature may be classified as nanoparticles.[2,14,19,39,43] In fact, some of the images presented in Figure 1 look more like large aggregates or ribbons, although closer inspection reveals that sometimes meshes of many tightly associated NF form.

The overall concentrations of surfactant and EDOT—not just their ratio—also have an effect on nanoparticle growth. A comparison between syntheses 5 and 7, which differ only in their total volume (10 vs. 15 mL water) show that diluting the solution appears to produce thinner fibers entangled in a mesh. Another factor that seems to control product morphology is the ratio of the SDS:$FeCl_3$. Fibers do not appear on their own (that is, without spherical aggregates) until the ratio of these two reactants, without respect to the EDOT concentration, is about 2 (syntheses 3, 4, 5, and 7). Longer, more dispersed fibers require a ratio closer to 3 (syntheses 1 and 6). Ratios much higher than this stay near the sphere realm (synthesis 8). This suggests that if the concentration of surfactant greatly outpaces the concentrations of the other solutions, there is insufficient material to fill out the template and the excess surfactant will group together in spherical aggregates. Much higher concentrations, as opposed to just ratios, also make longer fiber formation more difficult as it is more favorable to have many short fibers instead of longer ones.[13] This principle of surfactant and iron (III) chloride mediated growth where spheres formed is most clearly illustrated with synthesis 8.

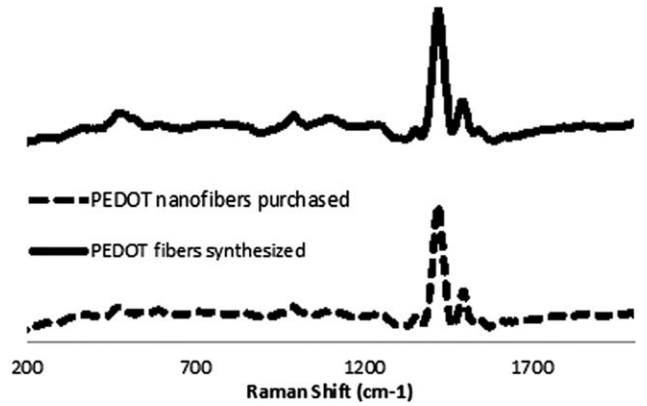

Figure 3. Raman spectrum of synthesized PEDOT NF compared to NF purchased commercially.

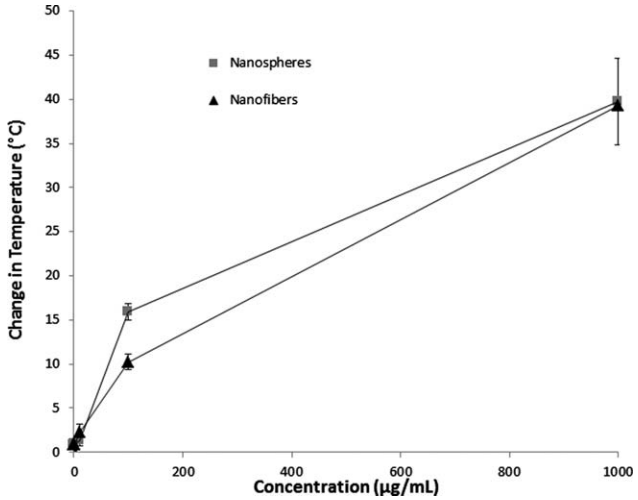

Figure 4. The change in temperature of 300 μL volumes of PEDOT NF or NS in water, at different concentrations and exposed to 3 W of 800 nm light for 60 s.

Optical and Thermal Properties

As Yoon *et al.* has previously shown, synthesis of PEDOT nanoparticles using soft templating leads to oxidation of the particles corresponding to strong NIR absorption due to polaron and bipolaron formation.[8] Polaron decay is ideal for enhancing the photothermal potential of PEDOT for medical use.[44–46] Both PEDOT NS and NF have broad optical absorption throughout the infrared region, as shown in Figure 2. The Raman spectrum of our synthesized NF, as shown in Figure 3, matches closely with the signature of commercially purchased PEDOT nanotubes, even though the commercial material has a more rounded "pillow-type" instead of tubular morphology. Based on polaron theory PEDOT NF should be capable of generating heat when stimulated with infrared light, and in this work an 800 nm diode laser was used to evaluate bulk temperature increases of an aqueous volume containing increasing concentrations of NF. As shown in Figure 4, both NS and NF generate heat when dispersed in aqueous media. For example, concentrations of NS at 10 μg/mL lead to a temperature increase of the solution of 1.3 °C and 10 μg/mL of NF lead to a 2.3 °C rise. At a concentration of 100 μg/mL the NS are superior, generating a 15.9 °C increase compared to NF's 10.2 °C. These temperatures are biologically relevant as a 7 °C increase above basal temperature would be 44 °C, which is in the range of mild hyperthermia and above which is above the thermal ablation threshold for tissue.

Cell Viability in PEDOT- Doped Tissue Phantoms

Addition of PEDOT NP may assist with orienting the collagen fibers as collagen polymerizes into a 3D matrix. Another benefit of adding conducting polymer nanoparticles to collagen gels is the potential for the particles to increase the electronic and ionic conductivity of the network in which the cells are growing.[39] As shown in Figure 5, neither the addition of 10 μg/mL NS nor NF exhibits any significant color change in the collagen

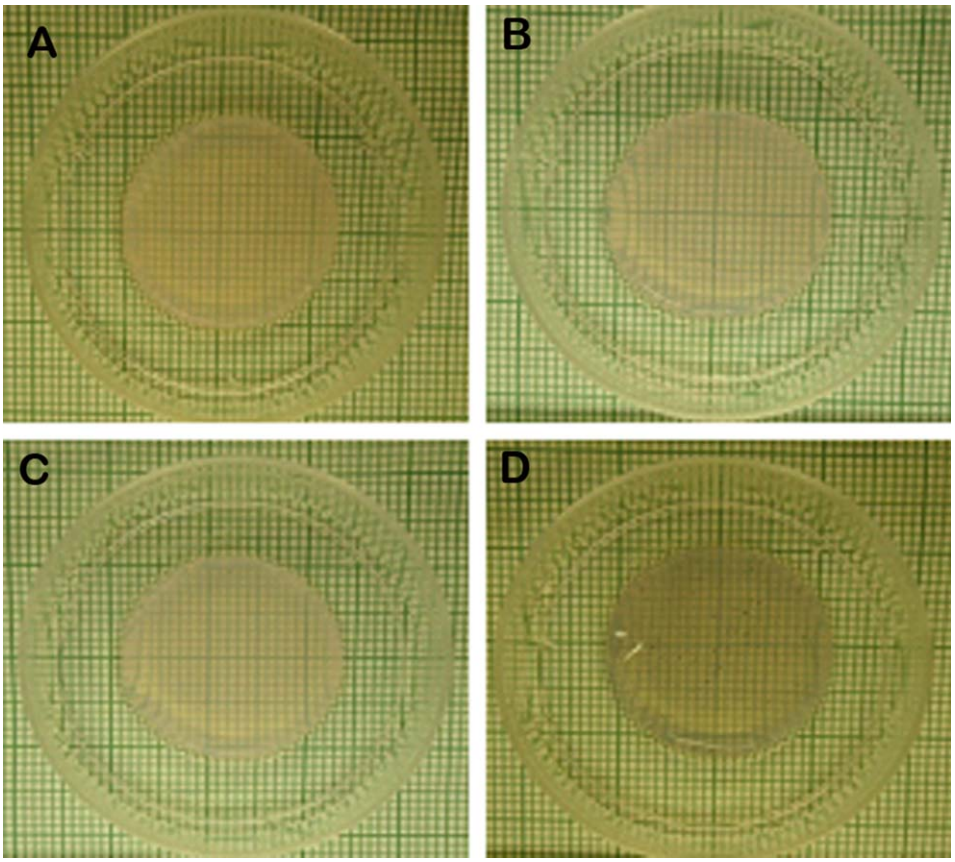

Figure 5. Collagen gels populated with one million HEPM cells and (A) no nanoparticles, (B) 10 μg/mL NS, (C) 10 μg/mL NF, (D) 100 μg/mL NF. [Color figure can be viewed in the online issue, which is available at wileyonlinelibrary.com.]

gels. However, addition of 100 μg/mL NF does lead to a visible darkening of the gels.

Upon consideration of the final results of the syntheses, the two dominant products were NF or NS. Syntheses 6 and 8 were chosen to best represent these groups respectively and then tested them *in vitro* to determine their cytocompatibility. The addition of surfactant Pluronic F127 to the collagen gel to help maintain dispersion of the nanoparticles most likely does not affect their morphology, as the concentration is very low (100 fold less than the amount of surfactant required for nanoparticle formation), and based on previous literature that conjugated polymer nanotubes and stable after formation and excess surfactant is inert.[11,47–49] Figure 6 shows that for the mouse

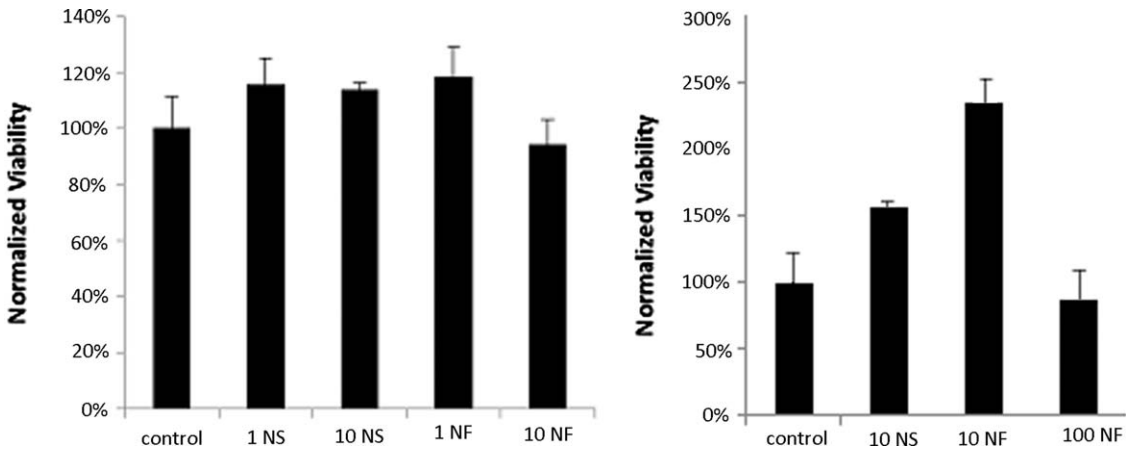

Figure 6. (A) Normalized viability of mouse cells cultured with PEDOT NF or NS (concentrations in μg/mL). The particles cause no change from the control in terms of viability, regardless of the aspect ratios or concentrations tested here. (B) Normalized viability of human cells cultured with PEDOT particles from syntheses 6 (NF) and 8 (NS). The increase in cell viability is due to the concentration, morphology and electrically conductive nature of the PEDOT NF.

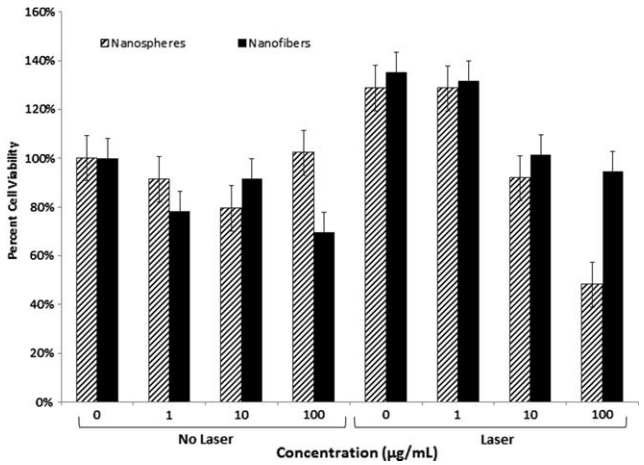

Figure 7. Viability of HEPM cells in 3-D collagen gels with increasing concentration of PEDOT NS or NF with and without exposure to 3 W of 800 nm light for 60 s.

cells, the particles show no difference from the control group regardless of the aspect ratio or 10-fold difference in concentration tested. The situation is similar with human cells, as previous work has shown that increasing concentrations of high aspect ratio electrically conductive particles can actually improve cell viability. The reason for the differences in cell viability between human and mouse cells is because of the size of the mouse versus human cells and their response to the nanometer sized of the nanoparticles. Increased cell viability in part B is most likely due to the HEPM cells responding to being cultured in the presence of the electrically conductive PEDOT NF. It has been documented in previous literature that nanofiber morphology and the conductive nature of the material can improve cell proliferation by mediating cell-cell communication.[39,40] To investigate this possibility, higher concentrations of the NF were evaluated. Figure 6 demonstrates that some concentrations of the particles can increase viability, but in the case of PEDOT particles it is unable to differentiate itself statistically from the control even if the concentration is quite high.

As shown in Figure 4, stimulation of the PEDOT nanoparticles generates heat that can be beneficial for clinical hyperthermia, for example ablation of diseased tissue. In an effort to gauge the effectiveness of PEDOT nanoparticles for killing cells in a three dimensional tissue phantom composed of collagen, HEPM cells were contained within the gels and the gels exposed to 800 nm light (3 W, 60 s). As shown in Figure 7, in the absence of infrared stimulation, the highest concentration (100 μg/mL) of PEDOT NF leads to a slight, yet not statistically significant decrease, in HEPM cell viability. Laser exposure increases the number of viable cells when no or 1 μg/mL of either PEDOT nanospheres or NF is used, as is commonly observed using this wavelength of light.[50] Although heat is generated by both types of PEDOT nanoparticles, and the NF actually have better infrared absorption than the NS, the NF are ineffective at reducing the number of viable cells compared to the NS. PEDOT NS may be most effective for photothermal cell killing as there is expected to be a higher number of nanoparticles to interface with the cells and transfer heat per mass amount compared to the NF.[47] Greater reductions in cell viability might also be able to be achieved by increasing the laser power or increasing the concentration of PEDOT nanoparticles in the tissue phantoms.

CONCLUSIONS

In conclusion, PEDOT nanoparticles with a variety of morphologies can be obtained using water only without the need for hexanes in the procedures. Nanoparticle shape and size is governed by an interaction of surfactant concentration with iron (III) chloride, and if the template has been disrupted or guided through physical stresses such as sonication or stirring. Generally, increasing surfactant concentration increases the propensity of fibers to form, while increasing the concentration of iron (III) chloride makes the particles less dependent on one another for stability. However, increasing surfactant concentration alone results once again in spheres. Sonication during template formation requires a higher concentration of surfactant to overcome the dissociation of the template, while slow stirring stretches the template and favors fiber formation. Regardless of whether NS or NF are generated, both types are cyto-compatible, and for some concentrations, increases the number of viable cells in a tissue phantom, most likely by enhancing the electrically conductive pathway and intercellular communication. The synthesized NS and NF are capable of generating hyperthermia and were evaluated in a three-dimensional tissue phantom, where NS were demonstrated to be more effective at cell ablation than NF.

ACKNOWLEDGMENTS

The authors would like to thank the Department of Plastic and Reconstructive Surgery for funding.

AUTHOR CONTRIBUTIONS

EMW, CMM, and NHL-P designed the experiments; EMW and CMM synthesized and characterized the nanoparticles; EMW and EM-L completed the tissue phantom and cell viability results. EMW, EM-L, and NHL-P wrote and revised the manuscript.

REFERENCES

1. Wan, M. X. *Adv. Mater.* **2008**, *20*, 2926.
2. Rumbau, V.; Pomposo, J. A.; Eleta, A.; Rodriguez, J.; Grande, H.; Mecerreyes, D.; Ochoteco, E. *Biomacromolecules* **2007**, *8*, 315.
3. Luo, S. C.; Yu, H. H.; Wan, A. C.; Han, Y.; Ying, J. Y. *Small* **2008**, *4*, 2051.
4. Darmanin, T.; Nicolas, M.; Guittard, F. *Langmuir* **2008**, *24*, 9739.
5. Zhang, X.; Lee, J. S.; Lee, G. S.; Cha, D. K.; Kim, M. J.; Yang, D. J.; Manohar, S. K. *Macromolecules* **2006**, *39*, 470.
6. Zhang, X.; MacDiarmid, A. G.; Manohar, S. K. *Chem. Commun. (Camb).* **2005**, *14*, 5328.
7. Musumeci, C.; Hutchison, J. A.; Samori, P. *Nanoscale* **2013**, *5*, 7756.
8. Yoon, H.; Hong, J. Y.; Jang, J. *Small* **2007**, *3*, 1774.
9. Garcia-Garcia, A.; Vergaz, R.; Algorri, J. F.; Quintana, X.; Oton, J. M.; Beilstein J. *Nanotechnol.* **2015**, *6*, 396.

10. Beckwith, K. S.; Cooil, S. P.; Wells, J. W.; Sikorski, P. *Nanoscale* **2015**, *7*, 8438.
11. MacNeill, C. M.; Wailes, E. M.; Levi-Polyachenko, N. H. *J. Nanosci. Nanotechnol.* **2013**, *13*, 3784.
12. Tian, B.; Zhang, X.; Yu, C.; Zhou, M.; Zhang, X. *Nanoscale* **2015**, *7*, 3588.
13. Tcacenco, C. M.; Zana, R.; Bales, B. L. *J. Phys. Chem. B* **2005**, *109*, 15997.
14. Paradee, N.; Sirivat, A. *Polym. Int.* **2014**, *63*, 106.
15. Burke, A.; Ding, X. F.; Singh, R.; Kraft, R. A.; Levi-Polyachenko, N.; Rylander, M. N.; Szot, C.; Buchanan, C.; Whitney, J.; Fisher, J.; Hatcher, H. C.; D'Agostino, R.; Kock, N. D.; Ajayan, P. M.; Carroll, D. L.; Akman, S.; Torti, F. M.; Torti, S. V. *Proc. Natl Acad. Sci. U.S.A.* **2009**, *106*, 12897.
16. Choi, J.; Yang, J.; Bang, D.; Park, J.; Suh, J. S.; Huh, Y. M.; Haam, S. *Small* **2012**, *8*, 746.
17. Fernandez Cabada, T.; de Pablo, C. S.; Serrano, A. M.; Guerrero Fdel, P.; Olmedo, J. J.; Gomez, M. R. *Int. J. Nanomed.* **2012**, *7*, 1511.
18. O'Neal, D. P.; Hirsch, L. R.; Halas, N. J.; Payne, J. D.; West, J. L. *Cancer Lett. [Article]* **2004**, *209*, 171.
19. Yue, Z.; Ren, X.; Dai, Q. Z. *Adv. Mater.* **2012**.
20. Abidian, M. R.; Kim, D. H.; Martin, D. C. *Adv. Mater.* **2006**, *18*, 405.
21. Alkilany, A. M.; Thompson, L. B.; Boulos, S. P.; Sisco, P. N.; Murphy, C. J. *Adv. Drug Deliv. Rev.* **2012**, *64*, 190.
22. Levi-Polyachenko, N. H.; Merkel, E. J.; Jones, B. T.; Carroll, D. L.; Stewart, J. H. *Mol. Pharm.* **2009**, *6*, 1092.
23. Liu, Z.; Chen, K.; Davis, C.; Sherlock, S.; Cao, Q. Z.; Chen, X. Y.; Dai, H. J. *Cancer Res.* **2008**, *68*, 6652.
24. Liu, Z.; Sun, X. M.; Nakayama-Ratchford, N.; Dai, H. J. *ACS Nano* **2007**, *1*, 50.
25. Melancon, M. P.; Elliott, A. M.; Shetty, A.; Huang, Q.; Stafford, R. J.; Li, C. *J. Controlled Release.* **2011**, *156*, 265.
26. Ren, F.; Bhana, S.; Norman, D.; Johnson, D.; Xu, J. L.; Baker, D. L.; Parrill, A.; Huang, L. X. *Bioconjug. Chem.* **2013**.
27. You, J.; Zhang, R.; Zhang, G.; Zhong, M.; Liu, Y.; Van Pelt, C. S.; Liang, D.; Wei, W.; Sood, A. K.; Li, C. *J. Control. Release.* **2012**, *158*, 319.
28. Weissleder, R. *Nat. Biotechnol.* **2001**, *19*, 316316.
29. Kim, J. B. editor. Three-Dimensional Tissue Culture Models in Cancer Biology. Seminars in Cancer Biology; Elsevier: **2005**.
30. Grinnell, F. *Trends Cell Biol.* **2003**, *13*, 264.
31. Lutolf, M.; Hubbell, J. *Nat. Biotechnol.* **2005**, *23*, 47.
32. Tomasek, J. J.; Gabbiani, G.; Hinz, B.; Chaponnier, C.; Brown, R. A. *Nat. Rev. Mol. Cell Biol.* **2002**, *3*, 349.
33. Sambale, F.; Lavrentieva, A.; Stahl, F.; Blume, C.; Stiesch, M.; Kasper, C.; Bahnemann, D.; Scheper, T. *J. Biotechnol.* **2015**, *205*, 120.
34. Shi, W. B.; Le, V. M.; Gu, C. H.; Zheng, Y. H.; Lang, M. D.; Lu, Y. H.; Liu, J. W. *J. Pharm. Sci.* **2014**, *103*, 1064.
35. Malarkey, E. B.; Fisher, K. A.; Bekyarova, E.; Liu, W.; Haddon, R. C.; Parpura, V. *Nano Lett.* **2008**, *9*, 264.
36. Bidez, P. R.; Li, S.; MacDiarmid, A. G.; Venancio, E. C.; Wei, Y.; Lelkes, P. I. *J. Biomater. Sci. Polym. Ed.* **2006**, *17*, 199.
37. Supronowicz, P.; Ajayan, P.; Ullmann, K.; Arulanandam, B.; Metzger, D.; Bizios, R. *J. Biomed. Mater. Res.* **2002**, *59*, 499.
38. Gilmore, K. J.; Kita, M.; Han, Y.; Gelmi, A.; Higgins, M. J.; Moulton, S. E.; Clark, G. M.; Kapsa, R.; Wallace, G. G. *Biomaterials* **2009**, *30*, 5292.
39. Abidian, M. R.; Corey, J. M.; Kipke, D. R.; Martin, D. C. *Small* **2010**, *6*, 421.
40. Richardson-Burns, S. M.; Hendricks, J. L.; Foster, B.; Povlich, L. K.; Kim, D. H.; Martin, D. C. *Biomaterials* **2007**, *28*, 1539.
41. Xu, J. H.; Zhen, H. J.; Jiang, Y. D.; Yang, Y. J. *J Wuhan Univ. Technol. Mater. Sci. Ed.* **2009**, *24*, 287.
42. Knaapila, M.; Evans, R. C.; Garamus, V. M.; Almásy, L.; Székely, N. K.; Gutacker, A.; Scherf, U.; Burrows, H. D. *Langmuir* **2010**, *26*, 15634.
43. Xiao, R.; Cho, S. I.; Liu, R.; Lee, S. B. *J. Am. Chem. Soc.* **2007**, *129*, 4483.
44. Di, B.; Meng, Y.; Wang, Y. D.; Liu, X. J.; An, Z. *J. Phys. Chem. B* **2011**, *115*, 9339.
45. Di, B.; Meng, Y.; Wang, Y. D.; Liu, X. J.; An, Z. *J. Phys. Chem. B* **2011**, *115*, 964.
46. Ouyang, J.; Xu, Q. F.; Chu, C. W.; Yang, Y.; Li, G.; Shinar, J. *Polymer* **2004**, *45*, 8443.
47. MacNeill, C. M.; Graham, E. G.; Levi-Polyachenko, N. H. *J. Polym. Sci. Part A: Polym. Chem.* **2014**, *52*, 1622.
48. Yoon, H.; Chang, M.; Jang, J. *Adv. Funct. Mater.* **2007**, *17*, 431.
49. Han, M. G.; Foulger, S. H. *Small* **2006**, *2*, 1164.
50. Lipovsky, A.; Oron, U.; Gedanken, A.; Lubart, R. *Lasers Med. Sci.* **2013**, *28*, 1113.